



Delineation of groundwater potential zones using cokriging and weighted overlay techniques in the Assin Municipalities of Ghana

Dennis Asante¹ · Emmanuel K. Appiah-Adjei¹ · Albert Asare¹

Received: 2 August 2021 / Accepted: 9 February 2022 / Published online: 3 March 2022
© The Author(s), under exclusive licence to Springer Nature Switzerland AG 2022

Abstract

This study has employed cokriging and weighted overlay techniques in a GIS environment to delineate groundwater potential zones from hydrogeological parameters in the Assin Municipalities, Ghana, where groundwater is the main source of potable water but access to it is less predictable since the aquifers are structurally controlled. Data from drilling logs, borehole development and construction, and pumping test on 67 boreholes in the area were utilized to estimate the hydrogeological parameters such as borehole yield, transmissivity, specific capacity, aquifer thickness and water strike elevation. Then, using the cokriging and weighted overlay techniques in ArcGIS, spatial thematic maps were created for all the parameters and integrated to produce the groundwater potential map, which categorized the study area into very low, low, moderate, and high groundwater potential zones. The results revealed that the cokriging technique was better in delineating the groundwater potential zones of the study area with a prediction accuracy of 67%, while the weighted overlay approach had an accuracy of 44%. However, the delineated moderate and high groundwater potential zones in the area for both approaches were largely the same and underlined by granitic rocks. Also, the generated groundwater potential map categorized approximately 0.1% (2.78 km²), 35.2% (850.45 km²), 43.6% (1054.62 km²) and 21.1% (509.15 km²) of the study area as very low, low, moderate and high groundwater potential zones, respectively. Thus, the study provides very useful information on groundwater potential zones delineation, which would aid in effective exploration and development of groundwater resources.

Keywords Cokriging · Weighted overlay · Groundwater potential · Hydrogeological parameters · Assin Municipalities

Introduction

Over 50% of global population depend on groundwater as the source of their drinking water (FAO 2002), whereas about 2.5 billion people worldwide depend solely on groundwater resources for their daily water needs (UNESCO 2012) due to its abundance, suitable natural quality, and availability in all seasons. In Ghana, groundwater serves as the main source of potable water for about 50% of the populace living in rural areas and it is increasingly becoming the only water source available to developing communities. Although it is known to be the most abundant freshwater resource globally, its availability for abstraction and sustainable use in an area depends on certain controlling factors including geologic media, hydrogeological properties, climatic conditions,

drainage pattern, topography, slope and land use/land cover (LULC) of the area. Thus, detailed investigations, ranging from remote sensing, geological, geophysical, and hydrogeological techniques, are required in identifying appropriate locations for sustainable abstraction of the resource in any area. This is to avoid loss of investments associated with drilling unsuccessful boreholes/wells, drying up of boreholes/wells in periods of prolonged absence of rainfall and, sometimes, unacceptable water quality (Kortatsi 1994; Xu and Usher 2006).

Hydrogeological studies such delineation of groundwater potential zones and groundwater modelling involve large volumes of multidisciplinary data (Gogu et al. 2001). Thus, Geographic Information Systems (GIS) has become a common tool used in such studies due to its suitability for handling complex geo-referenced data and applications in several disciplines including engineering and environmental studies (Stafford 1991; Goodchild 1993). Several researchers (Waikar and Nilawar 2014; Preeja et al. 2011; Yeh et al. 2009; Sener et al. 2005; Sikdar et al. 2004; Srinivasa

✉ Dennis Asante
dasante1.coe.ad@gmail.com

¹ Geological Engineering Department, Kwame Nkrumah University of Science and Technology, Kumasi, Ghana

and Jugran 2003; Jaiswal et al. 2003; Shahid et al. 2000; Krishnamurthy et al. 2000, etc.) have used remote sensing and GIS techniques in delineating groundwater potential zones in several parts of the world. Oh et al. (2011) used GIS and a probability model to map the probabilistic groundwater potential while Magesh et al. (2012) delineated groundwater potential zones using remote sensing, GIS and MIF techniques. On the other hand, other researchers have used integrated remote sensing, GIS and geoelectrical techniques (vertical electrical sounding, VES) to delineate groundwater potential zones where the VES was used to determine subsurface parameters such as aquifer resistivity, aquifer thickness, and depth to bedrocks (Chowdhury et al. 2009; Srivastava and Bhattacharya 2006; Israil et al. 2006; Sreedevi et al. 2005; Rao 2003; Shahid and Nath 2002; Murthy 2000; Edet and Okereke 1997). However, Todd (1980), as well as Jha and Peiffer (2006), stated that the existence of groundwater in an area can only be inferred from surface features such as geology, geomorphology, soils, land use/land cover, surface water bodies, drainage pattern, topographic slope, etc., which act as indicators of groundwater existence in remotely sensed data from satellite imagery since remote sensors cannot directly detect the presence of groundwater. As such, test drilling and stratigraphy analyses remain the most reliable and standard methods used for determining the location of aquifer, groundwater quality, physical characteristics of aquifers, etc. in an area (Chowdhury et al. 2009), although they are costly, time-consuming and require skilled manpower (Sander et al. 1996).

The use of GIS techniques in groundwater potential assessment varies considerably from one researcher to another. Whereas some researchers use the local influence of groundwater controlling parameters in assigning weights to different thematic layers prior to their integration for generation of groundwater potential map of an area (Nsiah et al. 2018; Gumma and Pavelic 2013), others use the Analytical Hierarchy Process (AHP) of the GIS-based multi-criteria decision analysis (MCDA) for the normalization of the assigned weights (Yifru et al. 2020; Arulbalaji et al. 2019; Andualem and Demeke 2019; Mallick et al. 2019; Bashe 2017; Hussein et al. 2017; Pinto et al. 2017; Shahid and Nath 2002). Also, the weighted overlay approach in groundwater potential delineation involves reclassification and weighting of the input thematic layers of the hydrogeological parameters prior to their integration. However, not all such parameters (e.g. aquifer zone thickness, fractured zone thickness, static water level, overburden thickness, etc.) have a standard classification scheme for such purpose. Hence, different researchers use different ranges of classification for the same parameters in different scenarios based on the local geology and some other hydrogeological consideration (Anteneh et al. 2021; Kumar et al. 2019; Nsiah et al. 2018; Akinlalu et al. 2017; Srinivasa and Jugran 2003; Jhariya et al. 2016),

which could be very subjective. Nonetheless, researchers including Zare et al. (2014) and Yalcin (2005) have reported that cokriging generally improves the prediction accuracy of spatial data interpolation. This is achieved by modelling the variogram of each parameter, and then the cross-variogram of the primary data/parameter and the covariate(s). Thus, cokriging makes use of secondary variables to improve upon the prediction accuracy (Yalcin 2005). As a result, Giraldo et al. (2020) used it to propose a model for predicting the environmental pollution of particulate matter considering wind speed curves as functional secondary variable. Hooshmand et al. (2011) also used cokriging in spatial estimation of groundwater quality parameters, whereas Ahmadi and Sedghamiz (2008), on the other hand, applied cokriging to map the groundwater depth. Similar works have been done by Hoeksema et al. (1989) Deutsch and Journel (1992), and Goovaerts (1997) using cokriging.

This study, therefore, delineates the groundwater potential zones in the Assin municipalities by integrating various hydrogeological parameters using both cokriging and the weighted overlay approaches in ArcGIS environment. The accuracy of groundwater potential maps generated by the two approaches are compared to determine the method that better predicts the groundwater potential of the area. The study area has over 85% of the population residing in rural areas with boreholes and protected hand-dug wells contributing over 90% of domestic water supplies (GSS 2012). Geologically, it is predominantly underlined by crystalline basin-type granitoids (GSA 2009) with a dense network of fractures (Ewusi and Kuma 2011); hence, the occurrence of groundwater in the area is less predictable. Thus, delineating the groundwater potential zones of the area is envisaged to provide useful prior information to aid in effective exploration and exploitation of the resource. Additionally, it would highlight areas where groundwater developers need to carry out more comprehensive groundwater exploration to avoid drilling unsuccessful boreholes and, thereby, safeguard their investments.

Materials and methods

Study area

The study area, located in the Central Region of Ghana (Fig. 1), consists of the Assin South, Assin Central and Assin North Municipalities, and lies within longitudes $5^{\circ} 20' N$ to $6^{\circ} 00' N$ and latitudes $1^{\circ} 06' W$ to $1^{\circ} 40' W$, covering a total land area of about 2417 km^2 . The main source of water for domestic purposes are boreholes fitted with hand pumps and protected Hand-Dug Wells (HDW), with pipe borne water contributing less than 10% (GSS 2012). Topography of the area is generally rolling to undulating with slopes trending

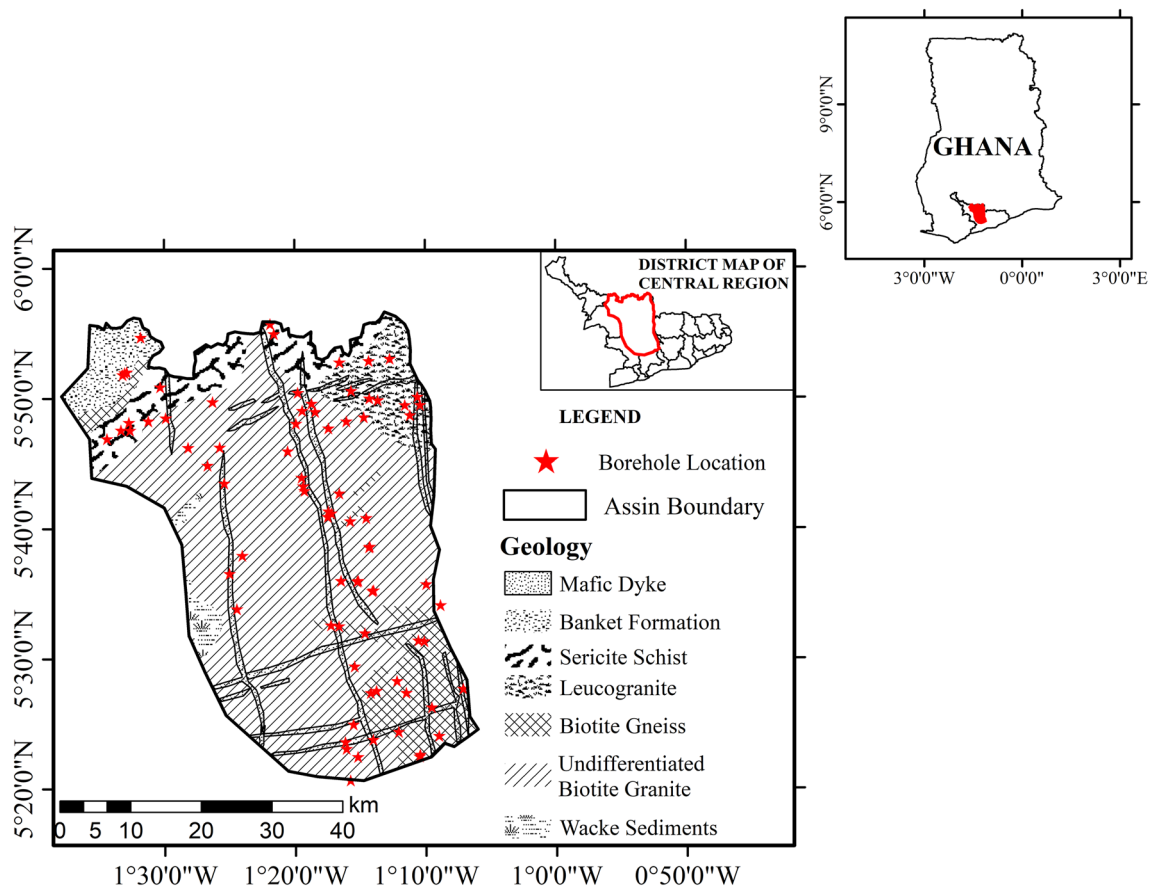


Fig. 1 Study area location with underlying geology and distribution of study boreholes

southwards from the Birim River, which is the main drainage system in the area and a major tributary of the Pra River (Asante-Annor et al. 2018). It falls within the evergreen and semi-deciduous forest zones with thick virgin forest in areas where there are forest reserves and lies within the semi-equatorial climate (Dickson et al. 1988), which is characterized by bimodal rainfall pattern (Asante-Annor et al. 2018).

Predominantly, the study area is made up of the Basin type granitoid of the Birimian System, covering about 90% of the area. The rock units found in the area include gneiss, granites and granodiorites with the gneissic rocks intruded by both acidic and basic igneous rocks such as white and pink pegmatite, aplite, granodiorite, and dolerite dykes (Gibrilla et al. 2010; Ganyaglo et al. 2010). The north-western portion of the area is made up of the Banket group of the Tarkwaian System consisting of rocks such as conglomerate, quartz pebble and quartzose sandstones (GSD 2009). Rocks in the study area have negligible primary porosity and permeability due to their crystalline nature; thus, groundwater flow is controlled by secondary geological structures such as fractures, joints and shear zones, and weathering in the rocks. Ewusi and Kuma (2011) indicated that weathering of the granitoids in the area is relatively thin, and dense

network of fractures are commonly found near the surface rather than at greater depths. However, the degree of weathering depends on the mineralogical composition of rocks, degree of fracturing and the rate of precipitation.

In general, the targets zones for groundwater development projects in the study area are weathered zones, rocks greatly affected by tectonic activity, contacts of intrusions, and highly fractured silica-rich and silicified rocks (Asante-Annor et al. 2018). However, the most productive area for groundwater is a formation with a combination of thick weathered zone and well-formed and highly persistent fracture network in the bedrock (Prackley 1984).

Data acquisition and database creation

Data on seventy-seven (77) boreholes drilled in the study area between the years 2006 and 2008 were acquired for the study from the Community Water and Sanitation Agency (CWSA) in Ghana. Pertinent information contained in the data included borehole location coordinates, borehole state (successful or unsuccessful), diameter and depth of borehole, geological drilling logs (from which parameters such as depth to bedrock, aquifer zone thicknesses, fractured zone

thickness, water strike, geology and lithologic description were determined), borehole development and construction with airlift yield information, pumping test data with static water levels, and water quality tests information. Overall, sixty-seven (67) of the drilled boreholes were successful (i.e., yields greater 13.5 L/min per CWSA guidelines), while the ten (10) were marginal to dry holes. The Mean Sea Level (MSL) was used as a common reference point in assessing the general variation of parameters such as static water level (SWL), water strike and depth to bedrock by subtracting them from their respective ground elevations to obtain the Static Water Elevation (SWE), Water Strike Elevation (WSE) and Bedrock Elevation, respectively.

The aquifer parameters like transmissivity, specific capacity, and maximum potential (sustainable) borehole yield were computed from the pumping test data. Each of the pumping tests was conducted over a 9 h duration, comprising 6 h of pumping at a constant rate followed by 3 h of recovery, in conformity with CWSA guidelines (CWSA 2010) and they were all single well tests. Due to well loss problems that is commonly associated with drawdown measurements in single well tests, data from the recovery phase of the pumping tests were used to estimate the Transmissivity (T) values following the Theis' (1935) recovery approach. Finally, the maximum potential (sustainable) yield of each borehole was computed using Eq. (1) proposed by van Tonder et al. (2000).

$$Q_{\text{Sustainable}} = (Q_{\text{Pumping}}/S_{\text{Pumping}}) \times S_{\text{Available}}, \quad (1)$$

where the ratio $Q_{\text{Pumping}}/S_{\text{Pumping}}$ is the specific capacity of the aquifer, with Q_{Pumping} being the discharge rate Q , and S_{Pumping} being the total drawdown at the end of the pumping. The available drawdown ($S_{\text{Available}}$) is given by Eq. (2):

$$S_{\text{Available}} = \text{Pump setting} - \text{SWL} - \text{buffer}. \quad (2)$$

A column of water called the buffer is always left above the pump setting beyond which the drawdown should not exceed. However, not all the borehole logs had the main water strike clearly indicated on them. Thus, for the sake of consistency and to ensure sustainable pumping of each borehole, a buffer of 3 m was used throughout in the determination of the sustainable borehole yields.

Generation of thematic maps of the hydrogeological parameters

Figure 2 shows the sequential order followed in the generation of thematic maps for hydrogeological parameters used in this study. Descriptive statistics such as the mean, mode, standard deviation, range, skewness, and kurtosis were computed for each hydrogeological parameter using SPSS version 20. The mathematical principles underlying

the interpolation method used for this study requires that the data be normally distributed. However, if the data distribution is otherwise, there are inbuilt mathematical functions to transform the data. Also, there should not be trends in the data to produce a more accurate interpolation surface. Hence, the histogram and Normal Quantile–Quantile (QQ) plot tools in ArcGIS were used together with the results from the data distribution analyses from the SPSS (skewness and kurtosis) to study the distribution of each hydrogeological parameter, whilst the trend analysis tool was used to determine whether trends exist in the data. Parameters that were not normally distributed were transformed using the appropriate mathematical module whereas those parameters that showed trends were corrected by removing them using the appropriate trend removal module.

Ordinary kriging interpolation technique was used to generate the spatial distribution layers for the individual hydrogeological parameters. Generally, geologic field data such as those used for this work are usually anisotropic in nature. However, several researchers (Eldeiry and Garcia 2012; Hu et al. 2005) have observed the usefulness of ordinary kriging interpolation technique in environmental interpolation mapping, groundwater quality assessment studies and soil science due to its ability to account for anisotropy in the dataset. Therefore, for the purpose of validating the above claim and for comparison, other kriging methods such as simple and universal kriging were also used to produce prediction maps of each parameter. It was, however, observed that the ordinary kriging produced a better interpolation surface.

The dataset for each parameter was randomly split into two (2) parts, each consisting of 70% training data, which was used in the creation of the prediction maps, and 30% test data used to validate the maps generated. The spatial autocorrelation of each dataset was predicted using the empirical semivariogram model of the geostatistical tool in ArcGIS software. In kriging, the model type used influences the output prediction surface as each model has been designed to fit different type of phenomena more accurately (ESRI 2016). Thus, the transformation and model type used for each parameter was based on the transformation—model type combination that produced the best prediction surface as per the results from validation and cross-validation. The performance of each model was assessed using both validation and cross-validation. In validation, the test data of a parameter was plotted on the geostatistical interpolation surface produced by each model. The predicted values for those points from the interpolated surface were then extracted using the “Extract to Points” tool in ArcGIS. The extracted predicted values were then compared with the measured test data values by determining the Pearson correlation coefficient (r) between them. Also, the accuracy of the generated surface for each parameter was determined by expressing the number of test data that fell within their exact zones on the

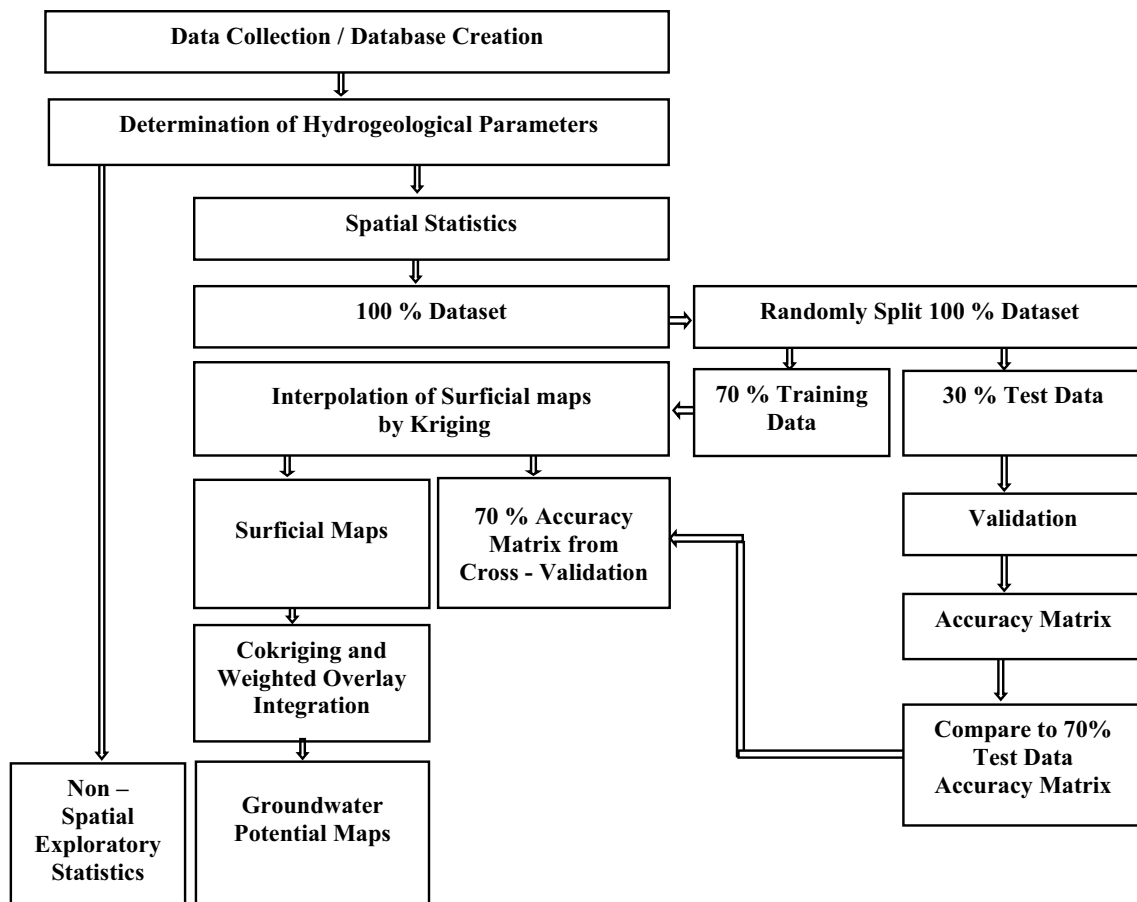


Fig. 2 The methodology followed in the generation of maps in the study area

generated prediction surface as percentage of the total test data. In the case of cross-validation, the mean standardized Error (ME), root mean square standardized error (RMSE), root mean square (RMS), and average standard error (ASE) were used to assess the performance of each model.

The groundwater potential map of the area was created using both Cokriging and the Weighted Overlay approaches to determine which method better predicted the groundwater potential of the study area. It has been established by number of researchers including Mohammed-Aslam et al. (2010) that there exists a positive correlation between borehole yield and availability of groundwater in any given area; hence, the Spearman's Correlation Coefficient (ρ) between borehole yield and each individual parameter was computed. The yield layer was used as primary variable of interest and integrated with different combinations of the other parameters that correlates well with the yield layer as covariates to produce the groundwater potential map of the study area using cokriging in ArcGIS.

In the weighted overlay approach, the interpolated thematic layers of the aquifer parameters were extracted into raster format in ArcGIS. The extracted raster layers were

then classified into their appropriate classes. The classification of the values of the input raster layers were based on specified scheme. For instance, categorization scheme for classifying the transmissivity raster layer was according to the Krasny's classification scheme (Krasny 1993), whereas that of the yield layer was according to the CWSA (2010) guidelines. The classified feature classes were then reclassified by ranking them on a scale of 1–5 based on the parameter's influence/indication of the availability of groundwater or otherwise, with 5 indicating the highest possibility of the presence of groundwater, whilst 1 indicates the least. Appropriate weights were then assigned to the reclassified raster layers based on their relative influence on the occurrence of groundwater and in accordance with similar research by Nsiah et al. (2018), and further integrated in ArcGIS to generate the composite groundwater potential maps using the various parametric combinations. For the sake of consistency, each of the parametric combinations used in cokriging was repeated in the weighted overlay approach. Additional potential maps were generated using the weighted overlay approach by adding more parameters to that used already to

determine its effect on the prediction accuracy of the generated potential maps.

Also, the weights assigned to the individual layers used in each of the models for the weighted overlay potential maps were varied until the ones that produced the best potential surface for each parametric combination as per the validation results were obtained. Table 1 shows the parametric combinations and the weights assigned to each reclassified raster layer in the generation of groundwater potential maps using the weighted overlay approach. The groundwater potential maps were validated by plotting the yield test dataset on each generated layer and expressing the number of data points that fell within the right zones delineated as low, moderate, high, and very high zones as a percentage of the total number of data points. Classification of yield values as low, moderate, high, etc. was in accordance with the guidelines provided by the Community Water and Sanitation Agency in their sector guidelines for small communities (CWSA 2010).

Results and discussion

Exploratory statistics of the aquifer parameters

Table 2 shows results for the non-spatial exploratory analyses of the hydrogeological data. Correlation between the ground elevation and bedrock elevation using the Spearman's Coefficient of correlation (ρ) shows a strong positive correlation (0.972), indicating high bedrock elevation in areas with high ground elevations and vice versa. This is confirmed by a weak negative correlation ($\rho = -0.291$) between overburden thickness and bedrock elevation, and thus, weathering effects on bedrock elevation in the area is minimal. Also, the borehole depth is not dependent on the depth of overburden. Though the thickness of overburden did not exceed 35 m, depth to fresh rock ranged from 12 to 55 m, having an average of about 35 m. Thus, on the average, about 20–25 m of the bedrock has undergone some level of alteration ranging from slight to moderate weathering. A very weak positive correlation ($\rho = 0.192$) exists between the fractured zone and the aquifer zone thicknesses contrary to water strike elevation and static water level, which have a strong positive correlation ($\rho = 0.926$). It was observed that the values of SWE are generally higher than their respective WSE, suggesting that the aquifers in the area are semi-confined to confined (Buckley 1986; Gibrilla et al. 2010). Both transmissivity and specific capacity datasets were right-skewed, with a moderate positive correlation ($\rho = 0.572$) between them. Borehole sustainable yield was also positively skewed and recorded the highest skewness among all the parameters. However, the borehole recovery dataset showed negative skewness (-0.66), indicating that most of

Table 1 Parametric combinations and the weights assigned to each layer

Map number	Parametric combination	Weight (%)
Map 1	Yield	40
	Specific capacity	25
	Transmissivity	25
	Static water level	10
Map 2	Yield	40
	Specific capacity	30
	Water strike	20
	Aquifer zone thickness	10
Map 3	Yield	40
	Specific capacity	25
	Transmissivity	20
	Aquifer zone thickness	15
Map 4	Yield	35
	Specific capacity	20
	Transmissivity	20
	Aquifer zone Thickness	15
	Water strike	5
	Total drawdown	5
Map 5	Yield	30
	Specific capacity	20
	Transmissivity	15
	Aquifer zone Thickness	10
	Static water elevation	10
	Overburden thickness	5
	Total drawdown	5
	Percentage recovery	5

the boreholes have recovery percentages greater than the mean value of 85%; hence, good for domestic water supply.

Results from the exploratory spatial statistics (Table 3) indicate that apart from specific capacity dataset, which had strong positive correlation ($\rho = 0.866$) with the yield dataset, all the other parameters showed weak to no correlation with the yield dataset. Nonetheless, transmissivity and SWL showed relatively better correlation with yield than the other parameters. Arguably, WSE, SWL and total draw-down datasets showed negative correlation with the yield dataset as expected. The cross-validation matrices (Table 3) from the various models produced ME values, which centred around zero (0) for all the parameters with the exception of SWL that produced a relatively higher ME value. In essence, negative values of ME for borehole depth, overburden thickness, water strike, SWL, specific capacity, and transmissivity models indicate underestimation of the errors in the prediction surface produced by their respective models, whereas positive ME values for all the remaining models are indication of overestimation of the errors. In the case of RMSE, almost all the models produced values closer to the

Table 2 Summary statistics for hydrogeological parameters

Parameter	Count	Mean	Median	Range	Standard deviation	Variance	Skewness	Kurtosis	No. of Outliers
Ground elevation (m)	77	148.48	149	57–200	26.95	726.76	−0.37	0.694	0
Borehole depth (m)	77	52.19	45	15–80	15.14	229.15	0.24	−0.92	0
Overburden thickness (m)	77	13.38	13	3–35	6.64	44.03	0.92	1.05	9
Bedrock elevation (m)	77	135.04	136	43–194	25.18	792.88	−0.33	0.76	1
Depth to fresh rock (m)	77	34.57	36	12–55	7.37	54.35	−0.43	1.35	3
Fractured zone thickness (m)	77	21.99	23	4–36	7.29	53.15	−0.08	−0.58	0
Aquifer zone thickness (m)	55	19.96	19	4–43	9.24	85.37	0.59	−0.31	0
Water strike (m)	59	30.63	28	12–62	10.4	108.10	1.34	2.07	4
Water strike elevation (m)	59	118.3	119.4	32.3–186.1	29.59	875.52	−0.2	0.33	1
Static water level (m)	36	7.10	6.12	1.1–25.60	5.39	29.05	1.64	3.09	3
Static water elevation (m)	36	144.1	144.5	84.7–197.0	28.57	816.03	0.12	−0.81	0
Total drawdown (m)	36	14.35	13.95	4.0–30.5	5.81	33.79	0.64	0.45	1
Percentage recovery (%)	36	86.26	89.73	58–100	13.72	188.37	−0.66	−0.86	0
Sustainable yield (L/min)	36	92.05	63.82	8.5–427.4	92.03	8469.05	1.84	3.86	2
Specific capacity (m ² /day)	36	4.98	3.49	0.3–16.9	4.54	20.65	1.27	0.66	2
Transmissivity (m ² /day)	36	6.27	3.15	0.1–28.2	7.19	51.77	1.72	2.54	2

Table 3 Accuracy matrices and validation results from kriging of each parameter

Parameter	ME	ASE	RMS	RMSE	<i>r</i>	Accuracy (%)
Borehole depth	−0.001	12.673	13.587	1.067	0.133	36.84
Overburden thickness	−0.027	7.526	6.295	0.815	0.000	61.11
Bedrock elevation	0.026	25.325	27.631	1.088	0.771	52.63
Depth to fresh rock	0.056	7.589	7.416	0.967	0.218	57.89
Fractured zone thickness	0.003	7.922	8.010	1.011	0.142	30.00
Water strike	−0.040	10.444	10.791	0.992	0.359	50.00
Aquifer zone thickness	0.003	9.640	9.413	0.977	0.434	42.86
Water strike elevation	0.015	25.979	28.255	1.050	0.413	57.14
Static water level	−0.154	6.798	6.686	1.101	−0.677	37.50
Static water elevation	0.046	31.335	33.063	1.050	0.262	37.50
Total drawdown	0.058	6.450	6.893	1.063	0.229	50.00
Percentage recovery	0.013	14.506	13.567	0.916	0.772	62.50
Sustainable yield	0.009	154.70	81.477	0.546	0.672	62.50
Specific capacity	−0.062	8.408	4.713	−0.706	0.197	77.78
Transmissivity	−0.010	58.268	10.556	0.292	−0.076	66.67

expected value of one (1) with only the sustainable yield and transmissivity models recording values, which moderately differed from one (1); thus, making the model prediction errors invalid. Models for all parameters recorded negligible difference between RMS and ASE (which is ideal for a well-fitted model) with the exception of sustainable yield and transmissivity models, which recorded considerable difference between their respective estimated RMS and ASE. Notwithstanding this, ASE < RMS for models of borehole depth, bedrock elevation, fractured zone thickness, water strike, WSE, SWE and total drawdown implies the models

underestimated the variability of the predicted values from the measured values. Contrary to this, the models for overburden thickness, depth to bedrock, aquifer zone thickness, SWL, percentage recovery, sustainable yield, specific capacity and transmissivity have ASE > RMS, indicating overestimation of the variability of the predicted values from the measured values. Bedrock elevation, percentage recovery and sustainable yield recorded a strong correlation between the predicted and measured test data values with percentage recovery recording the highest. Water strike, aquifer zone thickness and WSE recorded weak correlation between

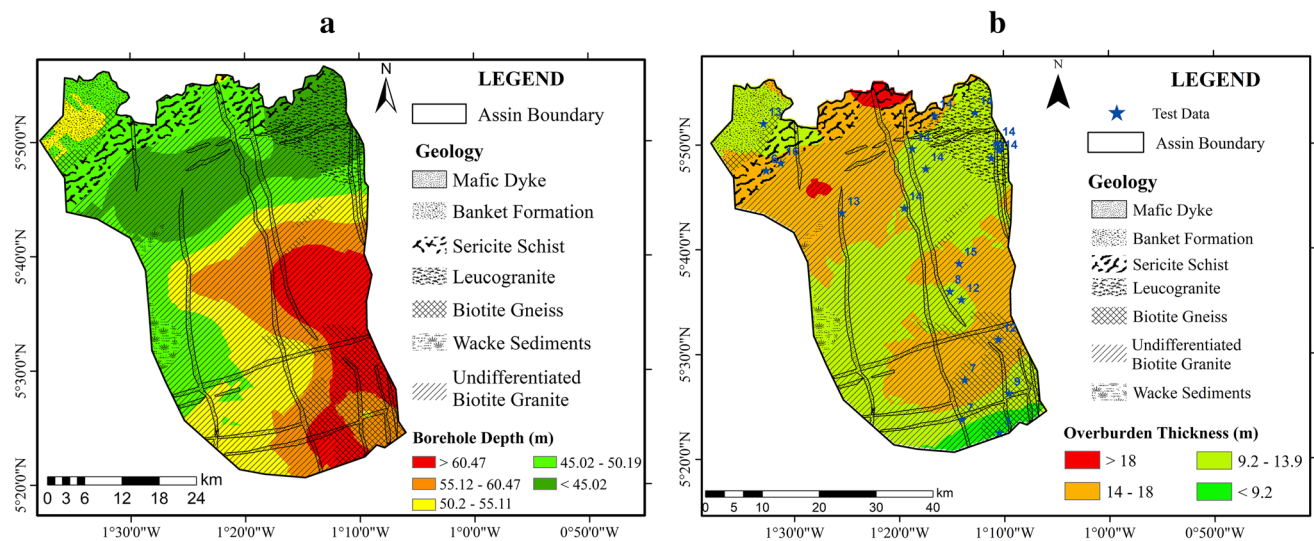


Fig. 3 Overlay of **a** borehole depth and **b** overburden thickness on the study area geology

the predicted and measured test data values, whereas all the remaining parameters recorded weak to no correlation between their respective measured and predicted values. There was no correlation between the measured and predicted test data values for overburden thickness whilst SWL recorded a negative correlation.

From the validation results, however, the specific capacity model had the best accuracy of 78% as opposed to the 63% of percentage recovery, which otherwise recorded the highest correlation coefficient between the predicted and measured test data values. Although the overburden thickness and transmissivity models each had no correlation between their measured and predicted test data values, each recorded an accuracy of over 60% from the validation. Also, bedrock elevation, aquifer zone thickness, percentage recovery and sustainable yield showed strong agreement between the correlation and validation results whereas water strike, WSE and SWE showed a moderate agreement.

Spatial evaluation of hydrogeological parameters

The depth range of boreholes (Fig. 3a) obtained in this study range from 15 to 80 m, which is consistent with ranges provided in other studies such as 35–90 m by Asante-Annor et al. (2018), 23–40 m by WRI (1992), and 15–100 by Armah (2000). Three distinct depth zones can be observed on the spatial variation plot of borehole depth, viz. ≤ 50 m, 50–60 m, and > 60 m. It is observed that the range of borehole depth in the northern part of the area is generally below 55 m. The zone with the shallowest depths is underlain by leucogranite and portions of the undifferentiated granitoids, which are parts of the granitoids of the Birimian supergroup.

The deepest boreholes are in areas underlain by the undifferentiated granitoids and the biotite gneiss.

Overburden thickness within the area is generally between 9 and 18 m with isolated patches of areas above 18 m and below 9 m, respectively, located around the northern portion underlain by the biotite gneiss and south-eastern part of the area (Fig. 3b). This range of values is consistent with that reported by Gibrilla et al. (2010) of between 4 and 20 m within the basin granitoids, which further attributes the wide range in overburden thickness to varying climatic conditions in the area. Gibrilla et al. (2011) noted that borehole yield in the intrusive granite complexes (granitoids) is generally low in areas where depth of weathering is shallow. Ewusi and Kuma (2011) and Ganyaglo et al. (2012) indicated that the depth of weathering is generally thicker in sedimentary and volcanic terranes as compared to granitoid terranes, which is not entirely the case in the current study. The depth of weathering in an area is, however, subject to climatic condition, particularly amount, distribution and frequency of rainfall, the extent and distribution of fractures and other structural discontinuities in the area (NRC 1996). Varying climatic conditions in the area (Gibrilla et al. 2011) and varying degree of structural discontinuities may, therefore, have caused the discrepancy above.

From Fig. 4a, it is observed that the north-western part of the area, underlain by the Banket group, recorded the lowest bedrock elevations. The granitoid terrains generally have bedrock elevations between 130 and 150 m above MSL, whereas the Birimian metasedimentary terrains (the sericite schist and biotite gneiss zones) have bedrock elevation of about 120–140 m above MSL. Three (3) distinct fractured zone thickness ranges can be observed in the study area, viz. ≤ 16.5 m, 16.5–23 m, > 23 m (Fig. 5a).

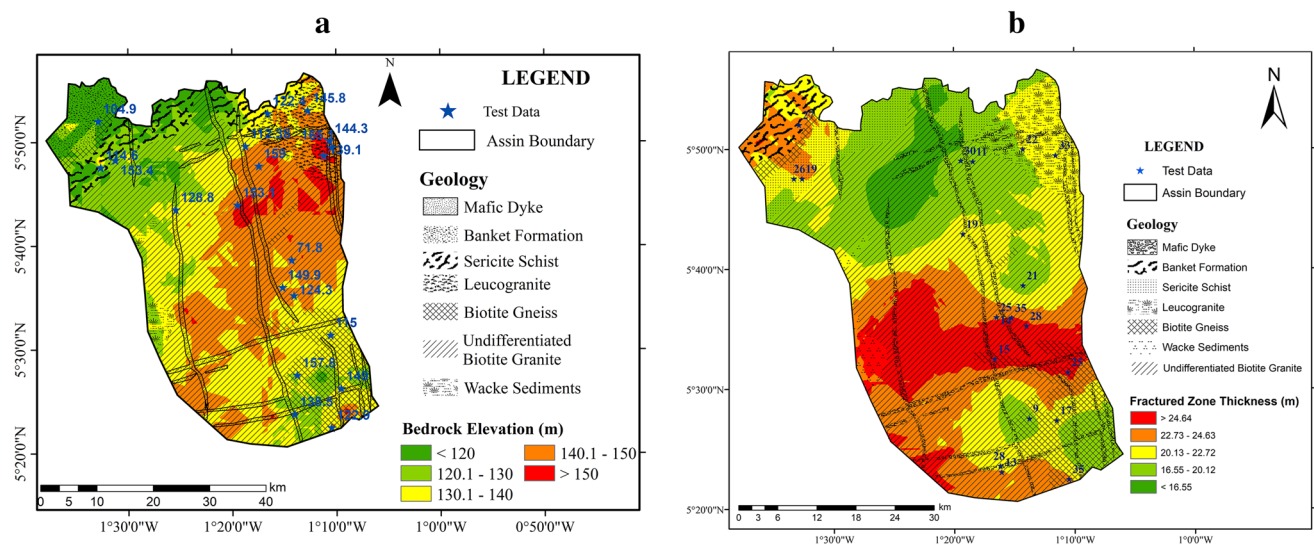


Fig. 4 Overlay of spatial distribution of **a** bedrock elevation, **b** fractured zone thickness on the study area geology

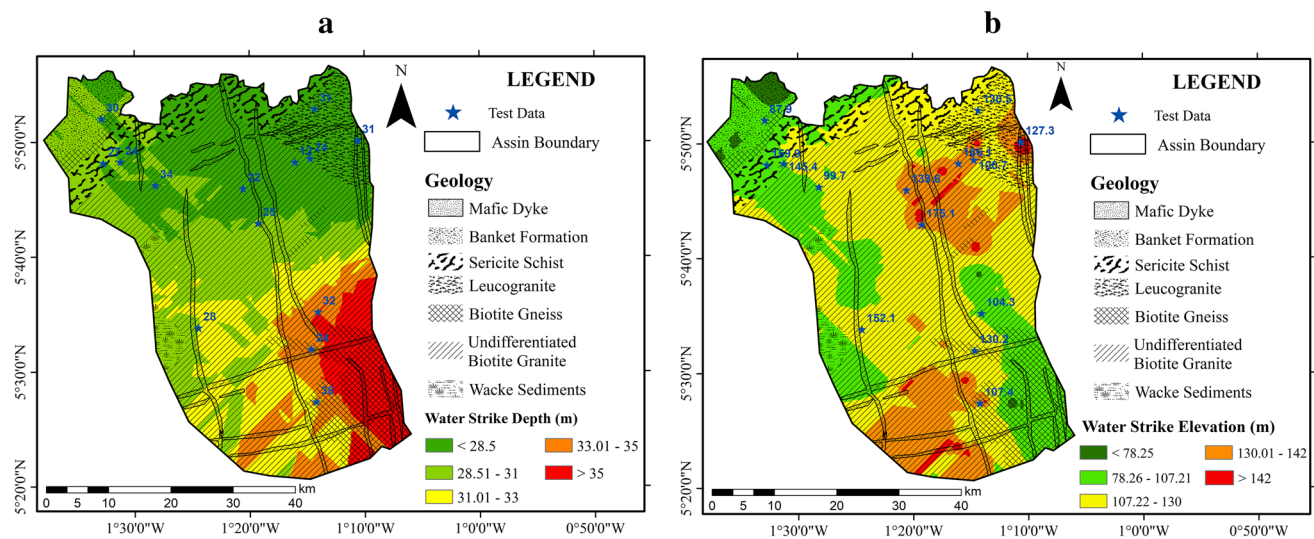


Fig. 5 Overlay of spatial distribution of **a** water strike depth and **b** water strike elevation on study area geology

Generally, all the thickness ranges can be found in the undifferentiated granite and the biotite gneiss terrains, whereas the Banket formation and the leucogranite zones have ranges of about 20–25 m and 16.5–23 m, respectively.

Depth at which water was struck in boreholes is generally high (generally > 30 m) at the south-eastern part of the area underlain by the biotite gneiss and undifferentiated biotite granite, and gradually decrease towards the western and north-eastern portions. Water strike in the undifferentiated granites, which covers the greater part of the area, is generally around 33 m or below whereas that of the leucogranite are below 28 m (Fig. 5a). As indicated on the borehole logs, water was encountered mainly in fractured zones during

drilling. Aquifers in crystalline rocks are mainly fractured zone aquifers and are developed at depth of about 20 m or more below ground surface (Gibrilla et al. 2011). Thus, the depth range of aquifers encountered in the area is consistent with values provided by Asante-Annor et al. (2018). Figure 5b is the elevation of the aquifers encountered in the area. It is observed that the deepest aquifers are at relatively lower elevations of 78–107 m above MSL. Gibrilla et al. (2011) stated that fractured zone aquifers in crystalline rocks tend to be localized in nature and, hence, groundwater occurrences are controlled by degree of fracturing and nature of groundwater recharge, whereas Ganyaglo et al. (2012) argued that fractured zone aquifers may be continuous or

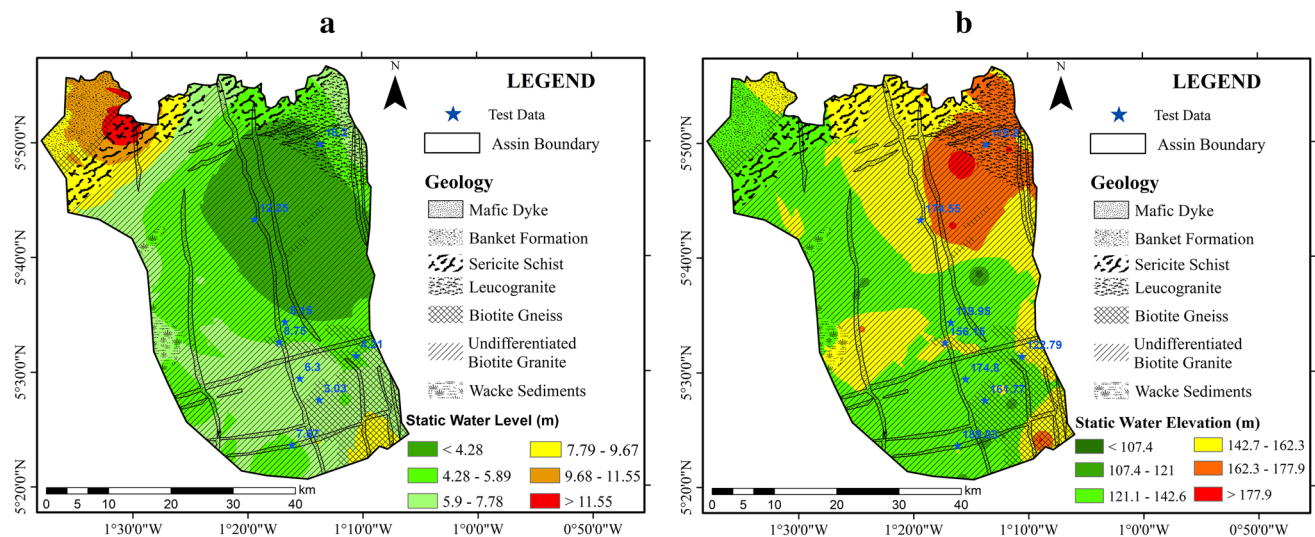


Fig. 6 Overlay of spatial distribution of **a** SWL and **b** SWE on the study area geology

discontinuous depending on the nature of the prevailing geological structures.

Generally, SWL in the area is less than 10 m, with a small localized area within the north-western corner underlain by sericite schist and the Banket formations having SWL values greater than 10 m (Fig. 6a). This range of values of SWL are consistent with the range of 1.09–14.75 m reported by Asante-Annor et al. (2018). It was observed in this study that across a given geological formation in the area, the SWL varies over just a small range. Figure 6b shows the spatial distribution of SWE in the area. Similar to the SWL, SWE does not show much variation over a given geological formation. Also, the pattern of distribution of SWE is similar to that of SWL since most of the areas with shallow SWL have relatively higher SWE. However, the spatial variation of the SWE is a bit more uniform compared to the SWL. The highest SWE values occurred around the north-eastern part of the area underlain by the leucogranites. Hence, given that there is a hydraulic connection, groundwater is expected to flow from this area towards the western and the southern parts of the study area.

Though the specific capacity values obtained ranges between 0.3 and 16.9 m³/day/m with a mean of 4.98 m³/day/m, spatial consideration indicates almost the entire area of having specific capacity ranging from 1 to 11 m³/day/m (Fig. 7a). A similar range of specific capacity values of 1.1–18.32 m³/day/m was recorded by Asante-Annor (2018). Again, it is observed that the area with relatively high specific capacity coincides with the high yield zone in Fig. 7b. Borehole yields are in the range of 8.5–427 L/min within the study area and is averagely 92.05 L/min. Asante-Annor et al. (2018) reported yields of 60–400 L/min with an average of 134.60 L/min. Nonetheless, it is worth knowing

that most of the borehole locations of the work of Asante-Annor et al. (2018) are within the granitoid zones delineated as high yield zones in the current research; hence, it could possibly be the reason for the apparent deviation in the lower limit of the range.

Prackley (1984) generally reported the borehole yields within the entire Cape Coast basin as 1.67–500 L/min with a mean of 33.33 L/min for the intrusive granites, and 11.66–150 L/min with a mean of 61.67 L/min for the Birimian. Geologically, the high yielding boreholes are located within the undifferentiated granite zones and parts of the biotite granite zones. The Banket formation, the sericite schist, the north-western part of the undifferentiated granites and the northern part of the leucogranite are the terrains that recorded low yields.

Transmissivity values were categorized using the Krasny's classification scheme (Krasny 1993) and the spatial distribution is shown in Fig. 7c. Generally, the transmissivity ranges from 0.1 to 28.2 m²/day with a mean value of 6.27 m²/day. A transmissivity range of 0.36–13.47 m²/day and a mean value of 3.03 m²/day were reported in an earlier work by Asante-Annor et al. (2018) in the area. It is observed that most of the areas with high borehole yields are also zoned within the areas delineated as the relatively high transmissive areas. Based on the Krasny's classification scheme, 33.26 km² (1.4%) of the area has very low transmissivity (0.1–1 m²/day) and, hence, can only sustain withdrawals for local water supply with limited consumption, 1502.01 km² (62.1%) of the area has low transmissivity (1–10 m²/day) and can sustain smaller withdrawals for local water supply (private consumption), whereas the remaining 881.73 km² (36.5%) has intermediate transmissivity (10–100 m²/day) and therefore suitable

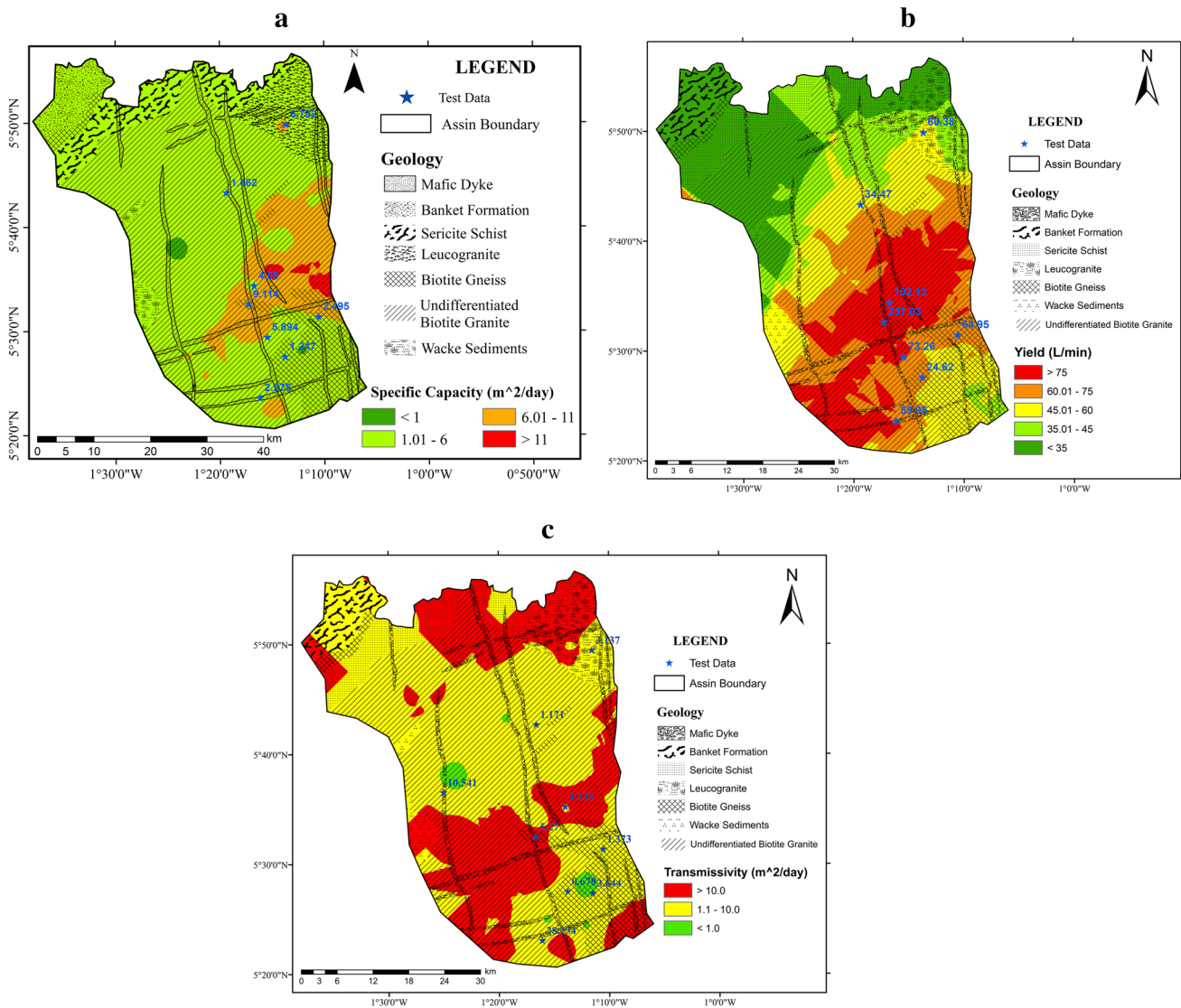


Fig. 7 Overlay of spatial distribution of **a** specific capacity, **b** borehole yield and **c** transmissivity on geological formations in the study area

for withdrawals for local water supply (small communities and plants).

Groundwater potential of the area

Table 4 shows the accuracy obtained for each parametric combination in cokriging and the weighted overlay approaches whilst Fig. 8a, b shows the potential maps generated. In all, the cokriging technique with the parametric combination of yield, specific capacity, transmissivity and static water level produced the best accuracy of 66.7% whilst its corresponding weighted overlay method had an accuracy of 44%. Generally, with the exception of the parametric combination of yield, specific capacity, water strike and aquifer zone thickness (Map 2), in which the performance

of cokriging yielded equal accuracy as the weighted overlay, cokriging relatively outperformed weighted overlay in each corresponding parametric combination. Also, it was observed (Table 4) that increasing the number of hydrogeological parameters in the weighted overlay approach had no improvement on the prediction accuracy of the potential maps, as in the case of Maps 4 and 5.

According to the CWSA borehole design guidelines for small communities (CWSA 2010), the minimum yield of a borehole to be considered for hand pump installation is 13.5 L/min while the minimum yield of a borehole to be considered for mechanisation is 85 L/min. However, depending on a comprehensive assessment of existing hydrogeological conditions, and an adequate technical evaluation of the yield of available boreholes, lower yields of up to 10 L/min and yields lower than 80 L/min may be considered for hand

pump installation and mechanization, respectively. Hence, in the creation and validation of the groundwater potential maps, areas with boreholes yields lower than 13.5 L/min were generally considered to have very low potential, areas with yields between 13.5 and 20 L/min were considered to have low potential, areas with yields between 20 and 50 L/min were considered to have moderate potential, those with yields between 50 and 100 L/min were deemed to have high potential, and areas with yields > 100 L/min considered to be of very high potential.

Thus, the groundwater potential of the area was generally categorised based on the cokrigging output as ranging from very low, through moderate-to-high potential (Fig. 8a). Spatial evaluation of this cokrigging output indicates that 2.78 km² representing 0.1% of the area has very low groundwater potential, 850.45 km² representing 35.2% has low potential, 1054.62 km² making up 43.6% of the area has moderate potential, and the remaining 21.1% with an area coverage of 509.15 km² has high potential. Similar to the cokrigging output groundwater potential map, the categories of groundwater potential of the area range from very

Table 4 Accuracy obtained for generated maps

Map number	Validation accuracy (%)	
	Cokrigging	Weighted overlay
Map 1	66.7	44
Map 2	33.3	33.3
Map 3	56	33.3
Map 4	–	33.3
Map 5	–	33.3

low through moderate to high for the weighted overlay output potential map (Fig. 8b). Thus, a total area of 9.01 km² (0.4%) has very low potential, 907.73 km² (37.6%) has low potential, 1148.53 km² (47.5%) has moderate potential and the remaining 351.73 km² (14.6%) has high potential per the overlay output. Geological evaluation of the generated potential maps shows that the undifferentiated granite zones have the highest groundwater potential ranging from low to high, whereas the biotite gneiss and leucogranites have low-to-moderate potential with the sericite schist and the Banket formation having low potential.

Discussion

The study area, predominantly underlain by crystalline intrusive granitic rocks of the Birimian system, is categorized into very low, low, moderate, and high groundwater potential zones by the integration of borehole yield, specific capacity, water strike and aquifer zone thickness using

cokrigging and weighted overlay approaches, with prediction accuracies of 66.7% and 44%, respectively. It is observed that aquifers in the area are mainly semi-confined to confined, which confirms earlier studies in the area by Buckley (1986) and Gibrilla et al. (2010). Exploratory spatial statistical analyses of the various hydrogeological parameters revealed that availability of groundwater (borehole yield) in the area highly correlates with specific capacity, but has moderate correlation with transmissivity as well as SWL. Other hydrogeological parameters such as overburden thickness, fractured zone thickness, etc., however, showed weak to no correlation with the borehole yield. This is consistent with results reported by Kanagaraj et al. (2019) in another area underlain by crystalline rocks with a combination of fractured and weather aquifer systems like the current study area.

On the other hand, a similar groundwater potential delineation study by Nsiah et al. (2018) in the sedimentary terrain of Nabogo basin showed borehole yields to be better correlated with regolith (overburden) thickness than SWL. This change may be attributed to the difference in geology and nature of aquifers in the two areas. Also, the spatial integration of hydrogeological parameters (i.e., borehole yield, regolith thickness, SWL and transmissivity) by Nsiah et al. (2018) using the weighted overlay approach produced a groundwater potential map of much higher prediction accuracy than in this study, which may also be to the difference in geology and aquifer nature in the areas.

Aside the use of hydrogeological parameters, Gumma and Pavelic (2013) integrated surficial parameters (i.e., geomorphology, geology, slope, drainage density, annual rainfall, land use/land cover, and soil type) using the weighted overlay approach to generate the groundwater potential map of Ghana, which had a good correlation with borehole yields. Though the study was on a country scale, the study categorized the area into three zones of poor, moderate, and good groundwater potential zones, which is consistent with the findings of the current study in a more localized scale. Similarly, the weighted overlay technique was a success in delineating groundwater potential zones in an area in India utilizing the surficial parameters (Mukherjee et al. 2012). Again, the weighted overlay technique has been used to integrate a combination of hydrogeological and surficial parameters for groundwater delineations in other studies (Kanagaraj et al. 2019; Al-Abadi et al. 2021, etc.), and it produced groundwater potential maps with prediction accuracy like this study.

Thus, it is observed that the parameters and the weighted overlay method of integration used in this study have been employed to successfully delineate groundwater potential zones in Ghana and other parts of the world, all of which yielded similar results. Though the cokrigging overlay approach produced maps of better prediction accuracy than the weighted overlay approach for the same parametric

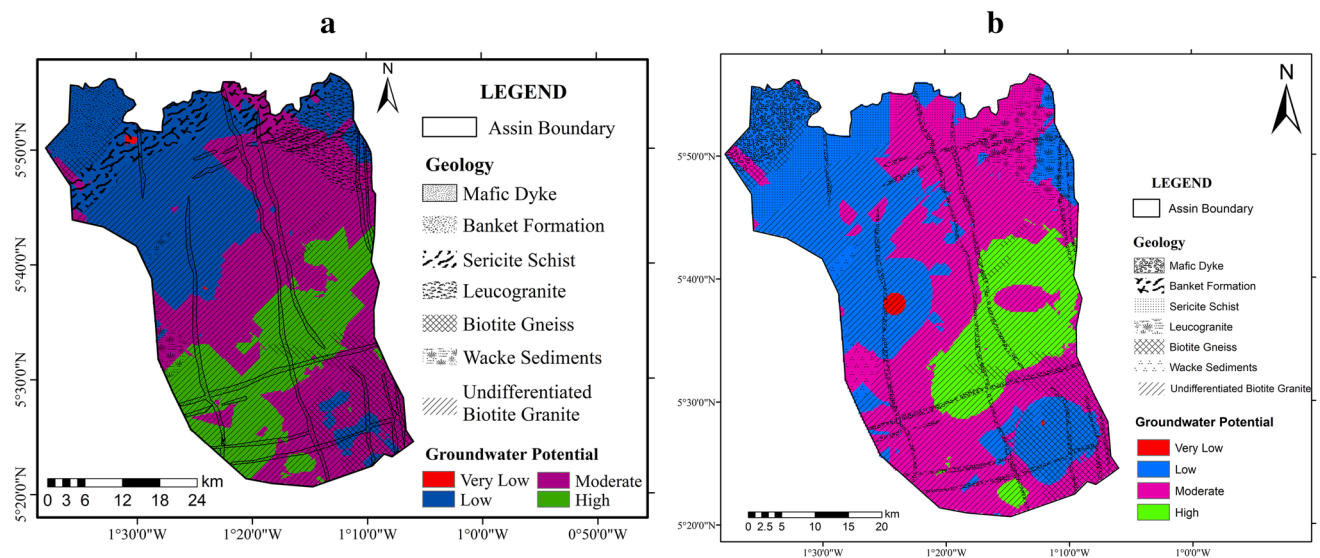


Fig. 8 Groundwater potential maps for the **a** cokriging and **b** weighted overlay approaches

combination, not much has been done on the method with respect to groundwater potential delineation.

Conclusion

This study has comprehensively assessed the groundwater potential of the Assin municipalities by generating groundwater potential maps of the area using cokriging and weighted overlay approaches in ArcGIS. It was observed that the cokriging technique produced maps with better prediction accuracy than the weighted overlay integration. Also, increasing the number of hydrogeological parameters in the weighted overlay approach had no improvement on the prediction accuracy of the potential maps.

Generally, borehole depth in the area ranges from 15 to 80 m with an average of 52 m, overburden thickness ranges from 9 to 18 m, the mean aquifer thickness is 19.96 m and the water strike from the ground level ranges from 12 to 62 m. Also, the yield of boreholes in the area ranges from 9 to 427 L/min with a mean of 92 L/min and their recovery rates after an hour are generally greater than 80%. Additionally, the specific capacity values in the area range from 0.3 to 16.9 m³/day/m with a mean of 4.98 m³/day/m whereas the transmissivity ranges from 0.1 to 28.2 m²/day with a mean value of 6.27 m²/day. Spatially, the groundwater potential of the study area varies from low to high with 850.45 km² (35.2%) of the area having low potential, 1054.62 km² (43.6%) possessing moderate potential, and 509.15 km² (21.1%) of the area having high potential based on the cokriging potential map. The weighted overlay potential map, on the other hand, indicates that a total area of 907.73 km² (37.6%) has low potential, 1148.53 km² (47.5%)

has moderate potential and 351.73 km² (14.6%) has high potential.

Geologically, the groundwater potential within the undifferentiated granitic terrains in the area range from low to high, the biotite gneiss and the leucogranites have low-to-moderate potential whereas the sericite schist and the Banket formation in the area have low groundwater potential. The study, therefore, offers very practical information on delineation of groundwater potential zones and is expected to guide in effective development of groundwater resources in the study area. It should, however, be noted that this study was conducted in an area underlain by crystalline basement rocks; hence, there may be variations in the outputs when the method is applied in areas underlain by different geology.

Acknowledgements Authors wish to thank Tullow Ghana for supporting this research through a graduate student scholarship. Again, the authors acknowledge Community Water and Sanitation Agency, Central Region, Ghana for making data available for the research.

Funding No funding was received for conducting this study.

Availability of data and materials The datasets generated during and/or analysed during the current study are available from the corresponding author on reasonable request.

Declarations

Conflict of interest The authors have no conflicts of interest to declare that are relevant to the content of this article.

References

- Ahmadi SH, Sedghamiz A (2008) Application and evaluation of Kriging and Cokriging methods on groundwater depth mapping. *Environ Monit Assess* 138:357–368
- Akinlalu AA, Adegbuyiro A, Adiat KAN, Akeredolu BE, Lateef WY (2017) Application of multi-criteria decision analysis in prediction of groundwater resources potential: a case of Oke-Ana, Ilesa Area Southwestern, Nigeria. *NRIAG J Astron Geophys* 6(1):184–200
- Al-Abadi AM, Fryar AE, Rasheed AA, Pradhan B (2021) Assessment of groundwater potential in terms of the availability and quality of the resource: a case study from Iraq. *Environ Earth Sci* 80(12):1–22
- Andualem TG, Demeke GG (2019) Groundwater potential assessment using GIS and remote sensing: a case study of Guna Tana Landscape, Upper Blue Nile Basin Ethiopia. *J Hydrol Reg Stud* 24:100610
- Anteneh Z, Alemu MM, Bawoke GK 1994 etnet, Kehali A, Fenta M, Desta MT (2021) Appraising groundwater potential zones using geospatial and multi-criteria decision analysis (MCDA) techniques in Andasa-Tul Watershed, Upper Blue Nile basin, Ethiopia. <https://doi.org/10.21203/rs.3.rs-309494/v1>
- Armah TK (2000) Groundwater salinization in parts of Southern Ghana. In: Oliver S (ed) *Groundwater: past achievements and future challenges*, (Proceedings of IAH Congress on Groundwater, 26 November 2000). A.A. Balkema Publication, Rotterdam. Pp 445–449
- Arulbalaji P, Padmalal D, Sreelash K (2019) GIS and AHP techniques-based delineation of groundwater potential zones: a case study from Southern Western Ghats India. *Sci Rep* 9(1):1–17
- Asante-Annor A, Acquah J, Ansah E (2018) Hydrogeological and hydrochemical assessment of basin granitoids in Assin and Breman Districts of Ghana. *J Geosci Environ Protect* 6(9):31–57
- Bashe BB (2017) Groundwater potential mapping using remote sensing and gis in Rift Valley Lakes Basin, Weito Sub Basin Ethiopia. *Int J Sci Eng Res* 8(2):43–50
- Buckley DK (1986) Report on advisory visit to water aid projects in Ghana. Unpublished Report, British Geological Survey, Hydrogeology Research Group, Wallingford
- Chowdhury A, Jha MK, Chowdary VM, Mal BC (2009) Integrated remote sensing and GIS-based approach for assessing groundwater potential in West Medinipur District, West Bengal India. *Int J Remote Sens* 30(1):231–250
- CWSA (Community Water and Sanitation Agency) (2010) *Small Community Sector Guidelines*. CWSA Publication, Accra
- Deutsch CV, Journel AG (1992) *Geostatistical Software Library and User's Guide*. New York, 119(147)
- Dickson KB, Benneh G, Essah RR (1988) *A new geography of Ghana*. Longman Group Ltd., London, p 34
- Edet AE, Okereke CS (1997) Assessment of hydrogeological conditions in basement aquifers of the Precambrian Oban Massif, Southeastern Nigeria. *J Appl Geophys* 36(4):195–204
- Eldeiry AA, Garcia LA (2012) Evaluating the performance of ordinary kriging in mapping soil salinity. *J Irrig Drain Eng* 138(12):1046–1059
- ESRI (Environmental Systems Research Institute) (2016). *ArcMap. How Kriging works*. Retrieved from <https://www.desktop.arcgis.com/en/arcmap/1.0.3/tools/3d-analyst-toolbox/how-kriging-works.htm#>. Accessed on 09 Jul 2021
- Ewusi A, Kuma JS (2011) Calibration of shallow borehole drilling sites using the electrical resistivity imaging technique in the Granitoids of Central Region Ghana. *Nat Resour Res* 20(1):57–63
- FAO (Food and Agriculture Organization of the United Nations). 2002. *Project Intégré Keita. Rapport Terminal du Project. Project GCP/NER/032/ITA*. Rome, FAO
- Ganyaglo SY, Banoeng-Yakubo B, Osae S, Dampare SB, Fianko JR, Bhuiyan MA (2010) Hydrochemical and isotopic characterisation of groundwater in Eastern Region of Ghana. *Water Resour Protect* 2:199–208
- Ganyaglo SY, Osae S, Dampare SB, Fianko JR, Bhuiyan MA, Gibrilla A, Osei J (2012) Preliminary groundwater quality assessment in the central region of Ghana. *Environ Earth Sci* 66(2):573–587
- Gibrilla A, Akiti TT, Osae S, Adomako D, Ganyaglo SY, Bam EPK, Hadisu A (2010) Origin of dissolve ions in groundwaters in the Northern Densu River Basin of Ghana Using stable isotopes of ^{18}O and 2H . *J Water Resour Prot* 2(12):1010–1019
- Gibrilla A, Bam EPK, Adomako D, Ganyaglo S, Osae S, Akiti TT, Kebede S, Achoribo E, Ahialey E, Ayanu G, Agyeman EK (2011) Application of Water Quality Index (WQI) and multivariate analysis for groundwater quality assessment of the Birimian and Cape Coast Granitoid Complex: Densu River Basin of Ghana. *Water Qual Expo Health* 3(2):63–78
- Giraldo R, Herrera L, Leiva V (2020) Cokriging prediction using as secondary variable a functional random field with application in environmental pollution. *Mathematics* 8(8):1305
- Gogu R, Carabin G, Hallet V, Peters V, Dassargues A (2001) GIS-Based hydrogeological databases and groundwater modelling. *Hydrogeol J* 9(6):555–569
- Goodchild MF (1993) The state of GIS for environmental problem-solving. In: Goodchild MF, Parks BO, Steyaert LT (eds) *Environmental modeling with GIS*. Oxford University Press, New York, pp 8–15
- Goovaerts P (1997) *Geostatistics for natural resources evaluation*. Oxford University Press on Demand
- GSA (Geological Survey Authority) (2009) *Geological Map of Ghana 1:1000000*, GSD, Accra, Ghana
- GSD (Geological Survey Department) (2009) *Geological Map of Ghana 1:1000000*, GSD, Accra, Ghana
- GSS (Ghana Statistical Service) (2012) *Population and Housing Census*. Ghana Statistical Service, Accra, Ghana
- Gumma MK, Pavelic P (2013) Mapping of groundwater potential zones across Ghana using remote sensing, geographic information systems, and spatial modeling. *Environ Monit Assess* 185(4):3561–3579
- Hoeksema RJ, Clapp RB, Thomas AL, Hunley AE, Farrow ND, Dearstone KC (1989) Cokriging model for estimation of water table elevation. *Water Resour Res* 25:429–438
- Hooshmand A, Delgh M, Izadi A, Amadali KA (2011) Application of Kriging and Cokriging in spatial estimation of groundwater quality parameters. *Afr J Agric Res* 6(14):3402–3408
- Hu K, Huang Y, Li H, Li B, Chen D, White RE (2005) Spatial variability of shallow groundwater level, electrical conductivity and nitrate concentration, and risk assessment of nitrate contamination in North China Plain. *Environ Int* 31(6):896–903
- Hussein AA, Govindu V, Nigusse AGM (2017) Evaluation of groundwater potential using geospatial techniques. *Appl Water Sci* 7(5):2447–2461
- Israil M, Al-Hadithi M, Singhal DC (2006) Application of a resistivity survey and geographical information system (GIS) analysis for hydrogeological zoning of a piedmont area, Himalayan Foothill Region India. *Hydrogeol J* 14(5):753–759
- Jaiswal RK, Mukherjee S, Krishnamurthy J, Saxena R (2003) Role of remote sensing and GIS techniques for generation of groundwater prospect zones towards rural development—an approach. *Int J Remote Sens* 24(5):993–1008
- Jha MK, Peiffer S (2006) Applications of remote sensing and GIS technologies in groundwater hydrology: past, present and future. BayCEER, Bayreuth
- Jhariya DC, Kumar T, Gobinath M, Diwan P, Kishore N (2016) Assessment of groundwater potential zone using remote

- sensing, GIS and multi criteria decision analysis techniques. *J Geol Soc India* 88(4):481–492
- Kanagaraj G, Suganthi S, Elango L, Magesh NS (2019) Assessment of groundwater potential Zones in Vellore district, Tamil Nadu, India using geospatial techniques. *Earth Sci Inf* 12(2):211–223
- Kortatsi BK (1994) Groundwater utilization in Ghana. IAHS Publications-Series of Proceedings and Reports-Intern Assoc Hydrological Sciences, 222, 149–156
- Krásný J (1993) Classification of transmissivity magnitude and variation. *Groundwater* 31(2):230–236
- Krishnamurthy J, Mani A, Jayaraman V, Manivel M (2000) Groundwater resources development in hard rock terrane—an approach using remote sensing and GIS techniques. *Int J Appl Earth Observ Geo-Inf* 2(3–4):204–215
- Kumar S, Machiwal D, Parmar BS (2019) A parsimonious approach to delineating groundwater potential zones using geospatial modeling and multicriteria decision analysis techniques under limited data availability condition. *Eng Rep* 1(5):2073
- Magesh NS, Chandrasekar N, Soundranayagam JP (2012) Delineation of groundwater potential Zones in Theni District, Tamil Nadu, using remote sensing GIS and MIF Techniques. *Geosci Front* 3(2):189–196
- Mallick J, Khan RA, Ahmed M, Alqadhi SD, Alsubih M, Falqi I, Hasan MA (2019) Modeling groundwater potential zone in a Semi-Arid Region of Aseer using fuzzy-AHP and geo-information techniques. *Water* 11(12):2656
- Mohammed-Aslam MA, Kondoh A, Rafeekh PM, Manoharan AN (2010) Evaluating groundwater potential of a hard-rock aquifer using remote sensing and geophysics. *J Spat Hydrol* 10(1):76–88
- Mukherjee P, Singh CK, Mukherjee S (2012) Delineation of groundwater potential zones in Arid Region of India—a remote sensing and GIS approach. *Water Resour Manag* 26(9):2643–2672
- Murthy KSR (2000) Groundwater potential in a semi-arid region of Andhra Pradesh—a geographical information system approach. *Int J Remote Sens* 21(9):1867–1884
- NRC (National Research Council) (1996) Rock fractures and fluid flow: contemporary understanding and applications. National Academies Press, Washington
- Nsiah E, Appiah-Adjei EK, Adjei KA (2018) Hydrogeological delineation of groundwater potential zones in the Nabogo Basin, Ghana. *J Afr Earth Sc* 143:1–9
- Oh HJ, Kim YS, Choi JK, Park E, Lee S (2011) GIS mapping of regional probabilistic groundwater potential in the area of Pohang City Korea. *J Hydrol* 399(3–4):158–172
- Pinto D, Shrestha S, Babel MS, Ninsawat S (2017) Delineation of groundwater potential zones in the Comoro Watershed, Timor Leste using GIS, remote sensing and analytic hierarchy process (AHP) technique. *Appl Water Sci* 7(1):503–519
- Prackley S (1984) The 30-well project. Internal Report, Catholic Diocese of Accra, Accra
- Preeja KR, Joseph S, Thomas J, Vijith H (2011) Identification of groundwater potential zones of a Tropical River Basin (Kerala, India) using remote sensing and GIS techniques. *J Indian Soc Remote Sens* 39(1):83–94
- Rao NS (2003) Groundwater prospecting and management in an agro-based rural environment of crystalline terrane of India. *Environ Geol* 43(4):419–431
- Sander P, Chesley MM, Minor TB (1996) Groundwater assessment using remote sensing and GIS in a rural groundwater project in Ghana: lessons learned. *Hydrogeol J* 4(3):40–49
- Sener E, Davraz A, Ozcelik M (2005) An integration of GIS and remote sensing in groundwater investigations: a case study in Burdur Turkey. *Hydrogeol J* 13(5–6):826–834
- Shahid S, Nath SK (2002) GIS integration of remote sensing and electrical sounding data for hydrogeological exploration. *J Spat Hydrol* 2(1)
- Shahid S, Nath S, Roy J (2000) Groundwater potential modelling in a soft rock area using a GIS. *Int J Remote Sens* 21(9):1919–1924
- Sikdar PK, Chakraborty S, Adhya E, Paul PK (2004) Land use/land cover changes and groundwater potential zoning in and around Raniganj Coal Mining Area, Bardhaman District, West Bengal—a GIS and remote sensing approach. *J Spat Hydrol* 4(2):1–24
- Sreedevi PD, Subrahmanyam K, Ahmed S (2005) Integrated approach for delineating potential zones to explore for groundwater in the Pageru River Basin, Cuddapah District, Andhra Pradesh India. *Hydrogeol J* 13(3):534–543
- Srinivasa Rao Y, Jugran DK (2003) Delineation of groundwater potential zones and zones of groundwater quality suitable for domestic purposes using remote sensing and GIS. *Hydrol Sci J* 48(5):821–833
- Srivastava PK, Bhattacharya AK (2006) Groundwater assessment through an integrated approach using remote sensing, GIS and resistivity techniques: a case study from a hard rock terrane. *Int J Remote Sens* 27(20):4599–4620
- Stafford DB (1991) Civil engineering applications of remote sensing and geographic information systems. In: A conference, (Proceedings of the Second National Specialty Conference, 14–16 May 1991). American Society of Civil Engineers
- Theis CV (1935) The relation between the lowering of the piezometric surface and the rate and duration of discharge of a well using ground-water storage. *EOS Trans Am Geophys Union* 16(2):519–524
- Todd DK (1980) Groundwater hydrology. Wiley, New York
- UNESCO (United Nations Educational, Scientific and Cultural Organization) (2012) World's Groundwater Resources are Suffering from Poor Governance. UNESCO Natural Sciences Sector News. Paris, UNESCO
- van Tonder G, Kunstmann H, Xu Y, Fourie F (2000) Estimation of the sustainable yield of a borehole including boundary information, drawdown derivatives and uncertainty propagation. In: Calibration and Reliability in Groundwater Modelling: Coping with Uncertainty, (Proceedings of the ModelCare'99 Conference Held in Zurich, Switzerland, 20–23 September 1999) IAHS Publications 265: 367
- Waikar ML, Nilawar AP (2014) Identification of groundwater potential zone using remote sensing and GIS technique. *Int J Innov Res Sci Eng Technol* 3(5):12163–12174
- WRI (World Resources Institute) (1992) World Resources, 1992–1993. Oxford University Press, New York
- Xu Y, Usher B (2006) Issues of groundwater pollution in Africa. In: By Y (ed) Groundwater pollution in Africa. Taylor & Francis, London, pp 3–9
- Yalcin E (2005) Cokriging and its effect on the estimation precision. *J South Afr Inst Min Metall* 105(4):223–228
- Yeh HF, Lee CH, Hsu KC, Chang PH (2009) GIS for the assessment of the groundwater recharge potential zone. *Environ Geol* 58(1):185–195
- Yifru BA, Mitiku DB, Tolera MB, Chang SW, Chung IM (2020) Groundwater potential mapping using SWAT and GIS-based multi-criteria decision analysis. *KSCE J Civ Eng* 24(8):2546–2559
- Zare CM, Zare CA, Malekian A, Bagheri R, Vesali SA (2014) Evaluation of different cokriging methods for rainfall estimation in Arid Regions (Central Kavir Basin in Iran). *Desert (BIABAN)* 19(1):1–9